Ocean Engineering 90 (2014) 34–38

Contents lists available at ScienceDirect

Ocean Engineering

journal homepage: www.elsevier.com/locate/oceaneng

Narrow ship wakes and wave drag for planing hulls

M. Rabaud *, F. Moisy

Laboratory FAST, Université Paris-Sud, CNRS. Bât. 502, Campus universitaire, 91405 Orsay, France

ARTICLE INFO

Article history:
Received 13 November 2013
Accepted 24 June 2014
Available online 14 July 2014

Keywords:
Wave drag
Planing hull
Kelvin wedge

ABSTRACT

The angle formed by ship wakes is usually found close to the value predicted by Kelvin, $\alpha = 19.47^\circ$. However we recently showed that the angle of maximum wave amplitude can be significantly smaller at large Froude number. We show how the finite range of wavenumbers excited by the ship explains the observed decrease of the wake angle as 1/Fr for $\mathrm{Fr} > 0.5$, where $\mathrm{Fr} = U/\sqrt{gL}$ is the Froude number based on the hull length L. At such large Froude numbers, sailing boats are in the planing regime, and a decrease of the wave drag is observed. We discuss in this paper the possible connection between the decrease of the wake angle and the decrease of the wave drag at large Froude number.

1. Introduction

A ship moving on calm water generates gravity waves presenting a characteristic V-shaped pattern. Lord Kelvin in 1887 was the first to explain this phenomenon and to show that the wedge angle is constant, independent of the boat velocity (see, e.g., Darrigol, 2005). According to this classical analysis, only the wavelength and the amplitude of the waves change with the velocity, and the half-angle of the wedge remains to be equal to 19.47°.

In contrast to this result described in many textbooks, we have shown recently that the apparent wake angle α, i.e. the angle of maximum wave amplitude, is not the Kelvin angle at large velocity, but rather decreases as 1/Fr, where $\mathrm{Fr} = U/\sqrt{gL}$ is the hull Froude number, based on the boat velocity U and on the waterline length L (Rabaud and Moisy, 2013). We have shown how this decrease can be simply modeled by considering the finite length of the boat. This scaling law $\alpha \propto 1/\mathrm{Fr}$ has recently received an analytical confirmation by Darmon et al. (2014).

Some years before Kelvin's work, William Froude, by towing model boats, observed that at intermediate velocity the hydrodynamic drag increases rapidly with the hull Froude number (Darrigol, 2005). Since then, the computation of hydrodynamic drag has received considerable interest (Michell, 1898; Tuck, 1989; Havelock, 1919), and still represents a challenge for naval architects. The wave drag (or wave-making resistance) R_W is the part of the hydrodynamic drag that corresponds to the energy radiated by the waves generated by the hull translation. For a displacement hull sailing at large velocity (Froude number in the range 0.2–0.5) the major part of the hydrodynamic drag is actually due to the wave drag.

In this paper we review some recent results about the Froude number dependence of the wake angle and the wave drag, and discuss the possible link between the decrease of these two quantities for planing sailing boats at large Froude number.

2. Wave pattern

When a boat sails on calm water at constant velocity U, the waves present around and behind the hull are only those that are stationary in the frame of reference of the boat. For a given wave of wavenumber k propagating in the direction θ with respect to the boat course (Fig. 1), this stationary condition gives

$$U \cos \theta(k) = c_\varphi(k) \tag{1}$$

where $c_\varphi(k)$ is the phase velocity of the wave.

Because of the dispersive nature of gravity waves, c_φ is a function of the wave number, $c_\varphi = \sqrt{g/k}$, implying that for a given propagation direction θ only one wavenumber is selected by Eq. (1):

$$k(\theta) = \frac{g}{U^2 \cos^2\theta}. \tag{2}$$

As a consequence, the smallest wave number (i.e. the largest wavelength) compatible with the stationary condition is $k_g = g/U^2$, and corresponds to waves propagating in the boat direction ($\theta = 0$). These so-called transverse waves are visible along the hull and following the boat.

Importantly, energy propagates at the group velocity and not at the phase velocity, and for gravity waves the group velocity is equal to half the phase velocity ($\mathbf{c_g} = \frac{1}{2}\mathbf{c}_\varphi$) (e.g., Lighthill, 1978).

* Corresponding author.
E-mail addresses: marc.rabaud@u-psud.fr (M. Rabaud), frederic.moisy@u-psud.fr (F. Moisy).

http://dx.doi.org/10.1016/j.oceaneng.2014.06.039
0029-8018/

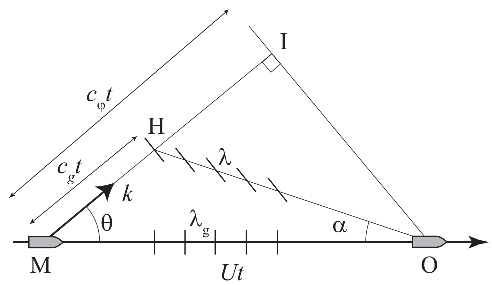

Fig. 1. Geometric construction of the wave pattern and angle definitions for a boat sailing at constant velocity U (Crawford, 1984).

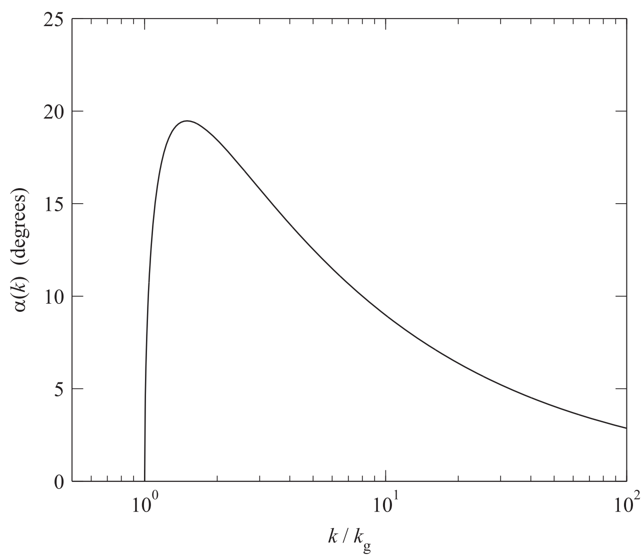

Fig. 2. Radiation angle $\alpha(k)$ as a function of the wavenumber ratio k/k_g (Eq. (3)), where $k_g = g/U^2$.

It follows from this ratio that the *radiation angle* $\alpha(k)$, along which the energy of a wavenumber k propagates in the frame of the disturbance, is given by (Keller, 1970; Rabaud and Moisy, 2013)

$$\alpha(k) = \tan^{-1}\left(\frac{\sqrt{k/k_g - 1}}{2k/k_g - 1}\right). \tag{3}$$

The plot of $\alpha(k)$ (Fig. 2) shows that for any given angle α smaller than 19.47° there are two possible values of k that correspond to two directions θ (Eq. (2)). One solution corresponds to transverse waves (smaller θ) and the other one to divergent waves (larger θ). The angle α takes its maximum value $\alpha_0 = 19.47°$ for $k_0/k_g = 3/2$, and no waves can be observed beyond this angle: this is the well known Kelvin angle, which corresponds to a cusp in the wave pattern. If the disturbance is a point source exciting a broadband spectrum of wavenumbers, then an accumulation of energy must take place at $k_0/k_g = 3/2$ (because the angular energy density $E(\alpha) = E(k)|\partial\alpha/\partial k|^{-1}$ diverges at k_0, with $E(k)$ the spectral energy density radiated by the disturbance), so the cusp is also the locus of maximum amplitude of the waves.

In reality, a boat cannot be described by a single point source: all the points of the hull act as wave sources and the detail of the amplitude of the wave depends on the exact shape, trim, sinkage of the hull, and on the Froude number. For example, for a poorly streamlined hull at low Froude number, two V-shaped wakes are visible, one originating from the bow and the other from the stern.

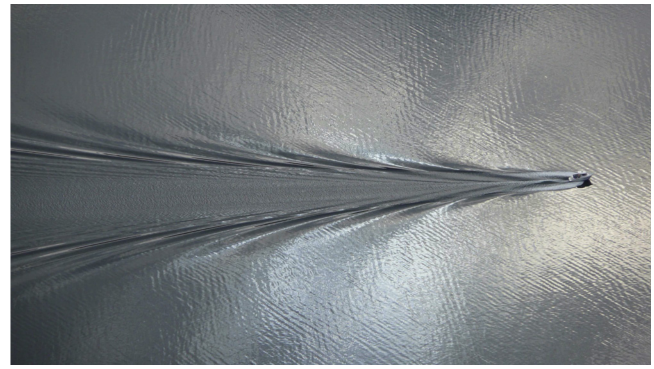

Fig. 3. Photograph of a fast planing motor-boat exhibiting a narrow wake (source: http://en.wikipedia.org/wiki/Wake).

In general the waves generated by a boat are characterized by a spectrum containing one or several characteristic length scales, corresponding to specific ranges of wavenumbers, so the maximum of wave amplitude is not necessarily located at the cusp angle (Lighthill, 1978; Carusotto and Rousseaux, 2013).

3. Wave angle for rapid boats

The commonly accepted result of Kelvin of a constant wake angle of 19.47° is called into question by numerous observations of significantly narrower wakes for planing boats at large velocity. This is illustrated in Fig. 3, showing a wake angle of order of 10°, significantly smaller than the Kelvin prediction.

Analyzing a set of airborne images from Google Earth©, we measured the wake angles and the Froude numbers for boats of various sizes and velocities. Using the scale provided on the images, we measured the overall length of the boat (assumed to be equal to the waterline length L) and the wavelength of the waves on the edge of the wake. From this wavelength the boat velocity U is determined using Eq. (2) and the Froude number is then computed. Our data clearly show a decrease of the wedge angle for Froude numbers larger than 0.5 (Fig. 2 of Rabaud and Moisy, 2013). Values as small as 7° were observed.

Wake angles smaller than the Kelvin prediction can be explained as follows. The key argument is that a moving disturbance of size L cannot excite efficiently the waves significantly smaller or larger than L. This is a general property of dispersive waves, analogous to the Cauchy–Poisson problem for the temporal evolution of an applied initial disturbance of characteristic size L at the free surface of a liquid (Havelock, 1908; Lighthill, 1978): the wave packet emitted by the disturbance travels at the group velocity $c_g = \frac{1}{2}\sqrt{g/k_f}$ corresponding to a wave number k_f of the order of L^{-1}, and the characteristic wavelength at the center of the wave packet is of the order of L. It is therefore possible to model the angle of maximum wave amplitude by simply considering that the energy radiated by the boat is effectively truncated below the wavenumber L^{-1}. At large boat velocity this wavenumber can be larger than the wavenumber $k_0 = 3g/2U^2$ which corresponds to the maximum Kelvin angle. Since only the wavenumbers of order of k_f are of significant amplitude, the angle of maximum wave amplitude is given by Eq. (3) evaluated at $k_f \simeq L^{-1}$. This simple model shows that the apparent wake angle is given by the Kelvin prediction as long as energy is supplied to k_0 (small Fr), but it is a decreasing function of velocity for Fr larger than a crossover Froude number Fr_c. Choosing $k_f = 2\pi/L$ (the exact prefactor depends on the shape of the disturbance spectrum) gives

$\mathrm{Fr}_c = \sqrt{3/4\pi} \simeq 0.49$, and an apparent wake angle decreasing as

$$\alpha \approx \frac{1}{2\sqrt{2\pi}\,\mathrm{Fr}} \tag{4}$$

for $\mathrm{Fr} \gg \mathrm{Fr}_c$ (the angle is given in radians). In other words, the Kelvin angle of 19.47° is always present at arbitrary Fr, but when $\mathrm{Fr} \gg \mathrm{Fr}_c$ the energy of the waves at 19.47° becomes negligible, and the energy emitted by the boat is preferentially radiated at the smaller angle given by Eq. (4). This law turns out to compare well with the wake patterns observed from airplane images. This is also consistent with the fact that at $\mathrm{Fr} > 0.5$ the transverse waves behind the boat ($\theta = 0$), which are visible for smaller Froude numbers, are no more visible (see Fig. 3), since their characteristic wavelengths fall outside the wave spectrum excited by the boat.

The decrease of the wake angle can be tested numerically. We follow the classical procedure of Havelock (1919) to evaluate the surface elevation field induced by an applied pressure field $P(x, y)$ at the water surface. The simplest choice is an axisymmetric Gaussian pressure distribution characterized by a single length scale L:

$$P(\mathbf{r}) = \frac{2\pi F_0}{L^2} \exp\left[-2\pi^2 \left(\frac{\mathbf{r}}{L} \right)^2 \right], \tag{5}$$

with $F_0 = \iint P(\mathbf{r})\, d^2\mathbf{r}$ the total applied force, which corresponds to the weight of the boat. Using linear potential theory, the resulting surface deformation $\zeta(x, y)$ can be computed as a Fourier integral (Lighthill, 1978; Raphaël and de Gennes, 1996; Darmon et al., 2014):

$$\zeta(\mathbf{x}) = -\lim_{\epsilon \to 0} \iint \frac{k\hat{P}(\mathbf{k})/\rho}{\omega(\mathbf{k})^2 - (\mathbf{k}\cdot\mathbf{U} - i\epsilon)^2} e^{i\mathbf{k}\cdot\mathbf{x}} \frac{d^2\mathbf{k}}{(2\pi)^2}, \tag{6}$$

where $\omega(\mathbf{k}) = \sqrt{g|\mathbf{k}|}$ and $\hat{P}(\mathbf{k})$ is the two-dimensional Fourier transform of $P(\mathbf{r})$. Wake patterns obtained by numerical integration of Eq. (6) for various Froude numbers are shown in Fig. 4 (the small parameter ϵ is chosen of order U/L_{box}, with L_{box} the domain size). These figures confirm the narrowing of the wake angle as Fr is increased, starting from a value close to the Kelvin prediction at Fr=0.5 and decreasing down to 4.9° at Fr=2.

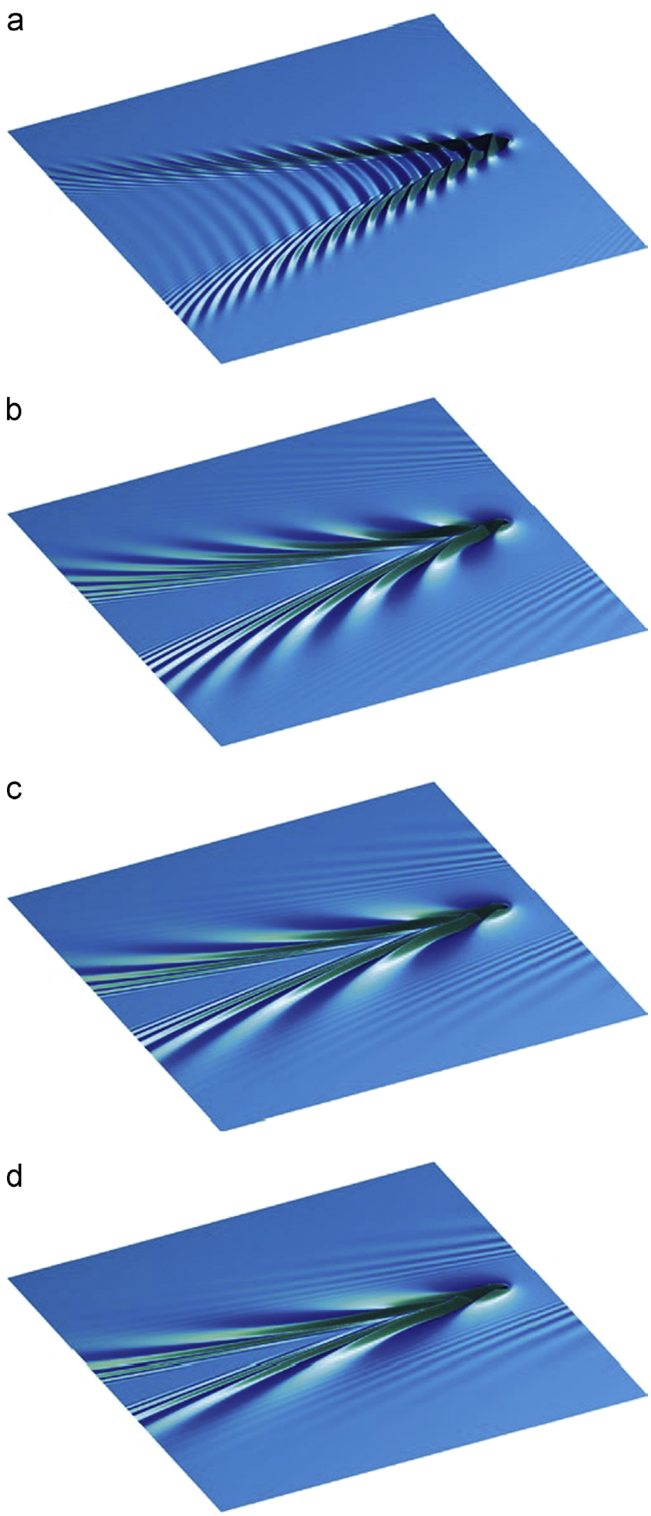

Fig. 4. Perspective views of the wave pattern generated by an axisymmetric (Gaussian) pressure distribution at various Froude numbers, Fr=0.5, 1, 1.5 and 2. The angle of maximum wave amplitude decreases from $\alpha \simeq 19$ to 4.9°. The wake patterns for $\mathrm{Fr} \simeq 1$–1.5 compare well with Fig. 3. (a) Fr=0.5, α=18.6°, (b) Fr=1.0, α=10.5°, (c) Fr=1.5, α=7.3° and (a) Fr=2.0, α=4.9°.

4. Wave drag

To describe the well known increase of the wave drag with the Froude number for displacement navigation at moderate Froude numbers ($\mathrm{Fr} < 0.5$) we first come back to Fig. 1, focusing on the transverse waves propagating in the boat direction ($\theta = 0$). These waves are the stationary waves observed along the side of the hull and behind the boat. Their wavenumber is given by Eq. (2), $k_g = g/U^2$, and their wavelength $\lambda_g = 2\pi/k_g$ can be written as $\lambda_g = 2\pi L\,\mathrm{Fr}^2$. This wavelength increases with velocity up to a particular velocity for which the wavelength is equal to the length of the boat. This velocity corresponds to $\mathrm{Fr} = 1/\sqrt{2\pi} \approx 0.4$. For this value the waves generated by the bow are in phase with the ones emitted at the stern and the draught (or sinkage) of the hull is maximum. This critical velocity is known as the hull limit speed, because around this Froude number the wave drag increases drastically and the trim of the boat starts to be strongly affected by the generated waves. We now know that this "limit speed" can be overcome with light and powerful boats as they reach the planing regime. In this regime of large Froude number, hydrodynamic lift can become significant, decreasing the immersed volume of the hull if the hull shape is well designed. It is often assumed that the observed decrease of the wave drag in the planing regime results from the smaller mass of fluid which needs to be pushed away by the hull. During this transition to planing, a significant acceleration of the boat can be observed. Note that the decrease of the wave drag at large velocity is often partly hidden by the increase of the other terms of the hydrodynamic drag, which typically increases as Fr^2.

We discuss now the possible connection between this wave drag decrease during planing and the decrease of the apparent wake angle described in the previous section. The wave drag R_W is

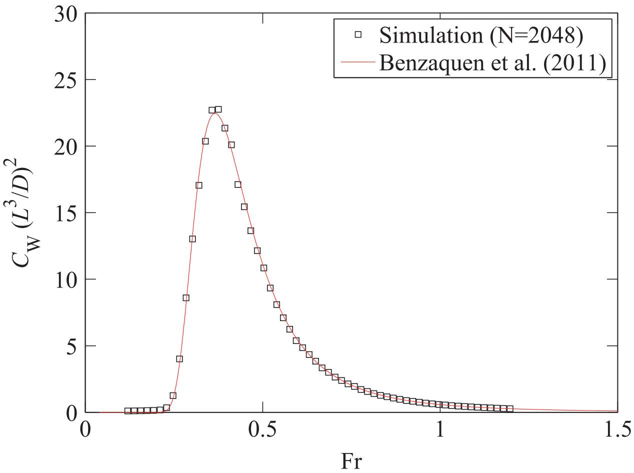

Fig. 5. Dimensionless wave drag calculated for a Gaussian moving pressure field with our simulated wave field (□) and comparison with Eq. (9) (—).

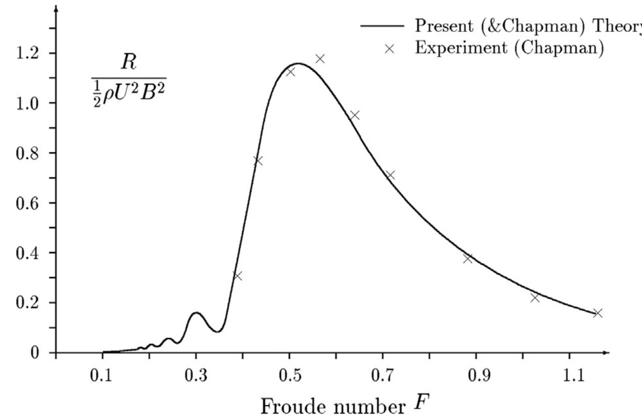

Fig. 6. Dimensionless wave drag for a parabolic strut (Tuck et al., 2002, Fig. 1).

the part of the hydrodynamic drag due to the energy radiated by the waves generated by the boat. In order to compare boats of different forms and displacement a dimensionless wave drag coefficient C_W is usually defined. Assuming hulls having all the same shape but not the same size, the wave drag only depends on the boat velocity U, waterline length L, gravity g and water density ρ. One finds by dimensional analysis

$$\frac{R_W}{\rho U^2 L^2} = C_W(\mathrm{Fr}). \tag{7}$$

In reality this coefficient C_W also depends on the exact shape of the boat, and alternate definitions where L^2 is replaced by LB or B^2 (where B is the beam of the hull) are also found in the literature. Another possibility is to build a dimensionless drag coefficient by normalizing the wave drag force R_W by the weight of the boat $F_0 = \rho g D$, where D is the static immersed volume of the hull. For a displacement boat, the wave drag coefficient rapidly increases (at least as Fr^4 if defined by Eq. (7)) and becomes the dominant part of the hydrodynamical drag at large Fr. Note that the power law $C_W \propto Fr^4$ can be recovered by a scaling argument, assuming that the amplitude of the waves scales as U^2 (using the Bernoulli relation) and that the wavelength observed along the Kelvin angle also scales as U^2 (Eq. (2)).

The wave drag for an applied pressure field can be computed by integrating the product of the pressure by the slope of the interface in the direction of the motion (Havelock, 1919):

$$R_W = \iint P(x,y)\frac{\partial \zeta}{\partial x}\,dx\,dy, \tag{8}$$

where $\zeta(x,y)$ is obtained by solving Eq. (6). Using the same Gaussian pressure field given by Eq. (5), we have computed the wave drag for various Froude numbers. The results, plotted in Fig. 5, are in perfect agreement with the exact result found by Benzaquen et al. (2011) for a Gaussian pressure field:

$$C_W = \left(\frac{D}{L^3}\right)^2 \frac{1}{\mathrm{Fr}^8}\int_0^{\pi/2} \frac{d\theta}{\cos^5\theta \exp\left[\left(\sqrt{2\pi}\,\mathrm{Fr}\,\cos\,\theta\right)^{-4}\right]} \tag{9}$$

This wave drag coefficient is maximum for $\mathrm{Fr} \simeq 0.37$, followed by a decrease as $C_W \simeq 1/\mathrm{Fr}^4$ at large Froude numbers. Interestingly, this maximum is very close to the critical Froude number $\mathrm{Fr}_c \simeq 0.49$ at which the wake angle starts decreasing. Both results are consequence of the finite extent of the wave spectrum excited by the disturbance: as the Froude number is increased, the surface deformation in the vicinity of the boat is no longer able to supply energy to the waves of wavelength $\lambda_g = 2\pi U^2/g$, resulting in a combined decrease of the wake angle ($\alpha \simeq 1/\mathrm{Fr}$) and of the wave drag ($C_W \simeq 1/\mathrm{Fr}^4$).

The overall shape of C_W computed by Eq. (9) is remarkably similar to the experimental curve of Chapman (1972) and computation by Tuck et al. (2002) (Fig. 6). This curve is usually interpreted as the result of the lift of the hull and the resulting decrease of the immersed volume at $\mathrm{Fr} > 0.5$. However, in our description, the prescribed pressure $P(x,y)$ does not depend on the velocity, so it does not contain the physics of the dynamical lift on the hull. This suggests that the dynamics of the planing and the associated decrease of the immersed volume are not necessary ingredients for the decrease of the wave drag at large Froude number. Such prediction could be tested in principle by towing a hull in a tank with imposed hull elevation and trim.

5. Conclusions

At large velocity many racing sailing boats are planing under the action of a strong hydrodynamic lift. The fact that the dynamically immersed volume is smaller than in the static condition provides a reasonable argument for the diminution of the wave drag. We propose here a complementary interpretation in which the combined decrease of the wave drag and of the apparent wake angle both follow from the finite extent of the wave spectrum excited by the ship. This interpretation is based on simulations of the wave pattern generated by an imposed pressure disturbance, that demonstrate that the narrow wake angles at large Froude number can be observed without lift and thus without planing regime (Rabaud and Moisy, 2013; Darmon et al., 2014). Although only axisymmetric disturbances are considered here, the Froude number dependence of the wake angle has been recently examined for non-axisymmetric disturbances by Noblesse et al. (2014) and Moisy and Rabaud (2014). The corresponding evolution of the wave drag is addressed in Benzaquen et al. (2014), providing an important step towards the connection between wave drag and wake angle for real boats.

We note that the present description is by construction limited to stationary motion, i.e. boat translating on a flat sea surface. In real situations the wind and thus the wind waves are usually large in planing conditions, and thus a periodic motion of the boat at the wave encounter frequency is observed. These non-stationary conditions are important because they increase the hydrodynamic drag when sailing at close reach (e.g., Seo et al., 2013) and decrease the drag when surfing on swell. However, this issue goes well beyond the scope of this paper.

References

Benzaquen, M., Chevy, F., Raphaël, E., 2011. Wave resistance for capillary gravity waves: Finite-size effects. Europhys. Lett. 96 (3), 34003.

Benzaquen, M., Darmon, A., Raphaël, E., 2014. Wake Pattern and Wave Resistance for Anisotropic Moving Objects. arXiv:1404.1699.

Carusotto, I., Rousseaux, G., 2013. The Cerenkov effect revisited: from swimming ducks to zero modes in gravitational analogs. In: Lecture Notes in Physics, vol. 870. Springer, Berlin (Chapter 6).

Chapman, R.B., 1972. Hydrodynamic drag of semisubmerged ships. J. Basic Eng. 72, 879–884.

Crawford, F.S., 1984. Elementary derivation of the wake pattern of a boat. Am. J. Phys. 52, 782–785.

Darmon, A., Benzaquen, M., Raphaël, E., 2014. Kelvin wake pattern at large Froude numbers. J. Fluid Mech. 738 (R3), 2014.

Darrigol, O., 2005. Worlds of Flow: A Hystory of Hydrodynamics from the Bernoullis to Prandtl. Oxford University, Oxford.

Havelock, T.H., 1908. The propagation of groups of waves in dispersive media, with application to waves on water produced by a travelling disturbance. Proc. R. Soc. Lond. Ser. A 81, 398.

Havelock, T.H., 1919. Wave resistance: some cases of three-dimensional fluid motion. Proc. R. Soc. Lond. Ser. A 95, 354–365.

Keller, J.B., 1970. Internal wave wakes of a body moving in a stratified fluid. Phys. Fluids 13 (6), 1425–1431.

Lighthill, J., 1978. Waves in Fluids. Cambridge University Press, Cambridge.

Michell, J.H., 1898. The wave resistance of a ship. Philos. Mag. Ser. 5 45, 106–123.

Moisy, F., Rabaud, M., 2014. Scaling of far-field wake angle of nonaxisymmetric pressure disturbance. Phys. Rev. E 89, 063004.

Noblesse, F., Jiayi, He, Yi, Zhu, Liang, Hong, Chenliang, Zhang, Renchuan, Zhu, Chi, Yang, 2014. Why can ship wakes appear narrower than kelvins angle? Eur. J. Mech. B/Fluids 46, 164–171.

Rabaud, M., Moisy, F., 2013. Ship wakes: Kelvin or Mach angle?. Phys. Rev. Lett. 110, 214503.

Raphaël, E., de Gennes, P.-G., 1996. Capillary gravity waves caused by a moving disturbance: wave resistance. Phys. Rev. E 53 (4), 3448.

Seo, M.-G., Park, D.-M., Yang, K.-K., Kim, Y., 2013. Comparative study on computation of ship added resistance in waves. Ocean Eng. 73, 1–15.

Tuck, E.O., 1989. The wave resistance formula of J.H. Michell (1898) and its significance to recent research in ship hydrodynamics. J. Aust. Math. Soc. Ser. B: Appl. Math. 30 (04), 365–377.

Tuck, E.O., Scullen, D.C., Lazauskas, L., 2002. Wave patterns and minimum wave resistance for high-speed vessels. In: The 24th Symposium on Naval Hydrodynamics, Fukuoka, Japan, 8–13 July 2002.